



Effect of bulk lubricant concentration on the excess surface density during R134a pool boiling[☆]

M.A. Kedzierski*

National Institute of Standards and Technology, Bldg. 226, Rm B114, Gaithersburg, MD 20899, USA

Received 30 June 2004; received in revised form 17 October 2004; accepted 1 November 2004

Available online 21 January 2005

Abstract

This paper investigates the effect that the bulk lubricant concentration has on the non-adiabatic lubricant excess surface density on a roughened, horizontal flat pool-boiling surface. Both pool boiling heat transfer data and lubricant excess surface density data are given for pure R134a and three different mixtures of R134a and a polyolester lubricant (POE). A spectrofluorometer was used to measure the lubricant excess density that was established by the boiling of an R134a/POE lubricant mixture on a test surface. The lubricant is preferentially drawn out of the bulk refrigerant/lubricant mixture by the boiling process and accumulates on the surface in excess of the bulk concentration. The excess lubricant resides in an approximately 40 μm layer on the surface and influences the boiling performance. The lubricant excess surface density measurements were used to modify an existing dimensionless excess surface density parameter so that it is valid for different reduced pressures. The dimensionless parameter is a key component for a refrigerant/lubricant pool-boiling model given in the literature. In support of improving the boiling model, both the excess measurements and heat transfer data are provided for pure R134a and three R134a/lubricant mixtures at 277.6 K. The heat transfer data show that the lubricant excess layer causes an average enhancement of the heat flux of approximately 24% for the 0.5% lubricant mass fraction mixture relative to pure R134a heat fluxes between 5 and 20 kW/m^2 . Conversely, both 1 and 2% lubricant mass fraction mixtures experienced an average degradation of approximately 60% in the heat flux relative to pure R134a heat fluxes between approximately 4 and 20 kW/m^2 . This study is an effort toward generating data to support a boiling model to predict whether lubricants degrade or improve boiling performance.

© 2004 Elsevier Ltd and IIR.

Keywords: Pool boiling; Horizontal surface; R134a; Lubricant; Polyolester; Correlation; Heat transfer; Density; Concentration

R134a: impact de la concentration du lubrifiant sur l'accroissement de la densité superficielle lors de l'ébullition libre

Mots clés : Ébullition libre ; Surface horizontale ; R134a ; Lubrifiant ; Polyolester ; Corrélation ; Transfert de chaleur ; Densité ; Concentration

[☆]Certain trade names and company products are mentioned in the text or identified in an illustration in order to adequately specify the experimental procedure and equipment used. In no case does such an identification imply recommendation or endorsement by the National Institute of Standards and Technology, nor does it imply that the products are necessarily the best available for the purpose.

* Tel.: +1 301 975 5282; fax: +1 301 975 8973.

E-mail address: mark.kedzierski@nist.gov.

0140-7007/\$35.00 © 2004 Elsevier Ltd and IIR.

doi:10.1016/j.ijrefrig.2004.11.007

Nomenclature	
<i>English symbols</i>	
A	absorbance
A_n	regression constant in Table 1 $n=0, 1, 2, 3$
c	concentration, mol/m ³
F	fluorescence intensity (percentage of pure lubricant signal)
F_c	fluorescence intensity from calibration (Eq. (1))
F_m	fluorescence intensity measured from boiling surface
h_{fg}	latent heat of vaporization of refrigerant, kJ/kg
I_o	incident intensity, V
I_t	transmitted intensity, V
k	thermal conductivity, W/m K
l	path length, m
l_a	thickness of lubricant bubble cap, m
l_c	thickness of excess layer, m
L_y	length of test surface, m
M_L	molar mass of lubricant, kg/mol
m	mass, kg
P	vapor pressure, kPa
P_c	critical pressure, kPa
P_r	reduced pressure (P/P_c)
q''	average wall heat flux, W/m ²
r_b	bubble departure radius, m
Ra_L	Rayleigh number based on projected area (Fig. 4)
T	temperature, K
T_w	temperature at roughened surface, K
U	expanded uncertainty
u_i	standard uncertainty
x	mass fraction of lubricant
y	test surface coordinate in Fig. 4, m
z	test surface coordinate in Fig. 4, m
<i>Greek symbols</i>	
β	temperature dependence of fluorescence coefficient, K ⁻¹
$\hat{\Gamma}$	dimensionless pool boiling refrigerant/lubricant excess surface density
Γ	lubricant excess surface density, kg/m ²
ΔT_s	wall superheat: $T_w - T_s$, K
ϵ	extinction coefficient, m ² /mol
ζ	fraction of excess layer removed per bubble
ρ	mass density of liquid, kg/m ³
σ	surface tension of refrigerant, kg/s ²
<i>English subscripts</i>	
b	bulk
e	excess layer
L	lubricant
m	measured, mixture
p	pure R134a
q''	heat flux
s	saturated state
T_w	wall temperature
v	vapor
<i>Superscripts</i>	
–	average

1. Introduction

The addition of lubricant to refrigerant can significantly alter the boiling performance due to lubricant accumulation at the heat transfer surface. Stephan [16] was one of the first researchers to note that a lubricant-rich layer exists near the tube wall. The excess concentration (excess surface density) arises from the low vapor pressure of the lubricant relative to

the refrigerant. The lubricant can be locally drawn out of solution as a consequence of refrigerant evaporation at the heat transfer surface. The refrigerant/lubricant liquid mixture travels to the heated wall, and the refrigerant preferentially evaporates from the surface leaving behind a liquid phase enriched in lubricant. A balance between deposition and removal of the lubricant establishes the thickness of the excess lubricant at the surface. It is hypothesized that the lubricant

Table 1

Estimated parameters for cubic boiling curve fits for plain copper surface $\Delta T_s = A_0 + A_1 q'' + A_2 q''^2 + A_3 q''^3$ ΔT_s in Kelvin and q'' in W/m²

Fluid	A_0	A_1	A_2	A_3
R134a				
3 K $\leq \Delta T_s \leq 6$ K	1.13413	5.40212×10^{-4}	-2.23805×10^{-8}	3.26420×10^{-13}
6 K $\leq \Delta T_s \leq 7$ K	5.08549	3.62330×10^{-5}	-1.57067×10^{-10}	2.86909×10^{-16}
R134a/DE589 (99.5/0.5) 3.6 K $\leq \Delta T_s \leq 8.5$ K	2.93162	1.46223×10^{-4}	-1.41993×10^{-9}	4.99448×10^{-15}
R134aa/DE589 (99/1) 11 K $\leq \Delta T_s \leq 21.5$ K	3.44201	2.16478×10^{-4}	-2.88547×10^{-9}	1.53149×10^{-14}
R134aa/DE589 (98/2)				
3 K $\leq \Delta T_s \leq 7$ K	-1.76162	1.53377×10^{-3}	-1.01205×10^{-7}	2.41953×10^{-12}
7 K $\leq \Delta T_s \leq 11$ K	6.91642	1.57640×10^{-5}	1.97728×10^{-10}	-5.36523×10^{-16}

excess layer controls the bubble size, the site density and, in turn, the magnitude of the heat transfer.

Kedzierski [6] developed a fluorescence measurement technique to verify the existence of the lubricant excess layer during pool boiling. A spectrofluorometer was specially adapted for use with a bifurcated optical bundle so that fluorescence measurements could be made perpendicular to the heat transfer surface. The study suggested that the excess layer was pure lubricant with a thickness ranging from 0.04 to 0.06 mm depending on the heat flux. The study examined only one R123/mineral oil mixture. Kedzierski [7] expanded the study by using the new technique to investigate the effect of three R123/mineral oil bulk concentrations on a mineral oil excess layer. The data for the three mixtures led to the development of a semi-theoretical model for predicting R123/lubricant mixture pool boiling heat transfer [4]. The model relies on excess surface density measurements and a dimensionless parameter representing the excess measurements. The present study uses the fluorescence measurement technique to extend the database to three R134a/polyolester lubricant (POE) mixtures to test and extend the dimensionless lubricant excess surface density parameter to other refrigerants and lubricants. Three different POE (DE589¹) mass compositions were investigated: 99.5/0.50, 99.02/0.98, and 98.04/1.96 (nominally 99.5/0.5, 99/1, and 98/2). The DE589 POE lubricant has a viscosity of 22 $\mu\text{m}^2/\text{s}$ at 313.15 K. The lubricant was chosen for its somewhat favorable fluorescence characteristics and its appropriate use with R134a.

2. Apparatus

Fig. 1 shows a schematic of the apparatus that was used to measure the pool boiling data of this study. More specifically, the apparatus was used to measure the liquid saturation temperature (T_s), the average pool-boiling heat flux (q''), the wall temperature (T_w) of the test surface, and the fluorescence intensity from the boiling surface (F). The three principal components of the apparatus were test chamber, condenser, and purger. The internal dimensions of the test chamber were 25.4 mm \times 257 mm \times 1.54 m. The test chamber was charged with approximately 7 kg of R134a from the purger, giving a liquid height of approximately 80 mm above the test surface. As shown in Fig. 1, the test section was visible through two opposing, flat 150 mm \times 200 mm quartz windows. The bottom of the test surface was heated with high velocity (2.5 m/s) water flow. The vapor produced by liquid boiling on the test surface was condensed by the brine-cooled, shell-and-tube condenser and returned as liquid to the pool by gravity.

Fig. 1 also shows the spectrofluorometer that was used to

make the fluorescence measurements and the fluorescence probe perpendicular to the heat transfer surface.

The fluorescence probe was a bifurcated optical bundle with 168 fibers spanning from the spectrofluorometer to the test surface. The 168 fibers of the probe were split evenly between the fibers to transmit the incident intensity (I_0) to the test surface and those to receive the fluorescence intensity (F) from the lubricant on the test surface. Further details of the test apparatus can be found in Refs. [6,8].

3. Test surface

Fig. 2 shows the oxygen-free high-conductivity (OFHC) copper flat test plate used in this study. The test plate was machined out of a single piece of OFHC copper by electric discharge machining (EDM). OFHC copper was chosen because of its well-known thermal conductivity and because its oxidation and wetting characteristics are expected to be similar to copper alloys used commercially with refrigerants. A tub grinder was used to finish the heat transfer surface of the test plate with a crosshatch pattern. Average roughness measurements were used to estimate the range of average cavity radii for the surface to be between 12 and 35 μm . The relative standard uncertainty of the cavity measurements were approximately $\pm 12\%$. Further information on the surface characterization can be found in Ref. [8].

4. Measurements and uncertainties

The standard uncertainty (u_i) is the positive square root of the estimated variance u_i^2 . The individual standard uncertainties are combined to obtain the expanded uncertainty (U), which is calculated from the law of propagation of uncertainty with a coverage factor. All measurement uncertainties are reported at the 95% confidence level except where specified otherwise. For the sake of brevity, only an outline of the basic measurements and uncertainties are given below. Complete detail on the heat transfer measurement techniques and uncertainties can be found in Refs. [9,10].

4.1. Heat transfer

All of the copper-constantan thermocouples and the data acquisition system were calibrated against a glass-rod standard platinum resistance thermometer (SPRT) and a reference voltage to a residual standard deviation of 0.005 K. Considering the fluctuations in the saturation temperature during the test and the standard uncertainties in the calibration, the expanded uncertainty of the average saturation temperature was no greater than 0.04 K. Consequently, it is believed that the expanded uncertainty of the temperature measurements was less than 0.1 K.

¹ A model polyolester made for NIST by ICI to investigate the bounds of property effects on heat transfer.

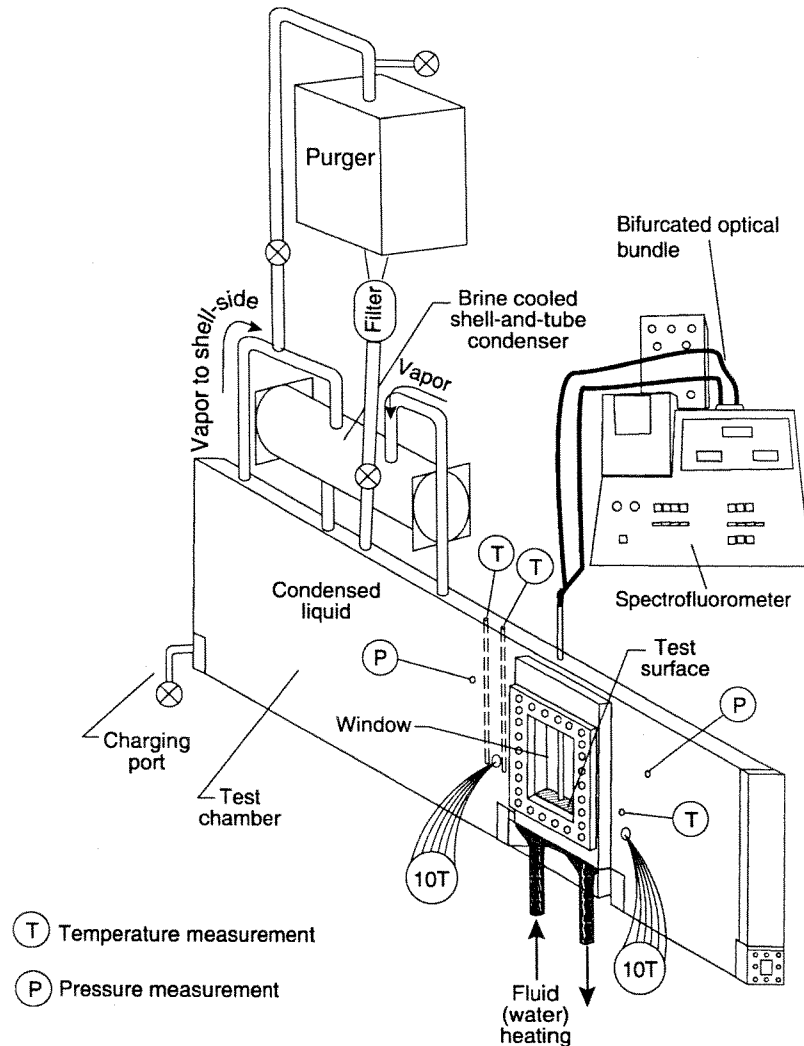


Fig. 1. Schematic of test apparatus.

Twenty 0.5 mm diameter thermocouples were force fitted into the wells of the side of the test plate shown in Fig. 2. The heat flux and the wall temperature were obtained by regressing the measured temperature distribution of the block to the governing two-dimensional conduction equation (Laplace equation). In other words, rather than using the boundary conditions to solve for the interior temperatures, the interior temperatures were used to solve for the boundary conditions following a backward stepwise procedure given in Ref. [11]. Fourier's law and the fitted constants from the Laplace equation were used to calculate the average heat flux (q'') normal to and evaluated at the heat transfer surface based on its projected area. The average wall temperature (T_w) was calculated by integrating the local wall temperature (T). The wall superheat was calculated from T_w and the measured temperature of the saturated liquid (T_s). Considering this, the relative expanded

uncertainty in the heat flux ($U_{q''}$) was greatest at the lowest heat fluxes, approaching 8% of the measurement at 10 kW/m². In general, the $U_{q''}$ was relatively constant between 4 and 5% for heat fluxes above 25 kW/m². The average random error in the wall superheat (U_{T_w}) was between 0.02 and 0.08 K. Plots of $U_{q''}$ and U_{T_w} versus heat flux can be found in Ref. [5].

4.2. Fluorescence

Ref. [6] describes the method for calibrating the emission intensity measured with the spectrofluorometer and the bifurcated optical bundle as shown in Fig. 1 against the bulk lubricant mass fraction. As outlined in Ref. [5], the excitation and emission wavelengths for the spectrofluorometer were experimentally determined as 394 and 467 nm, respectively. One modification was done to the

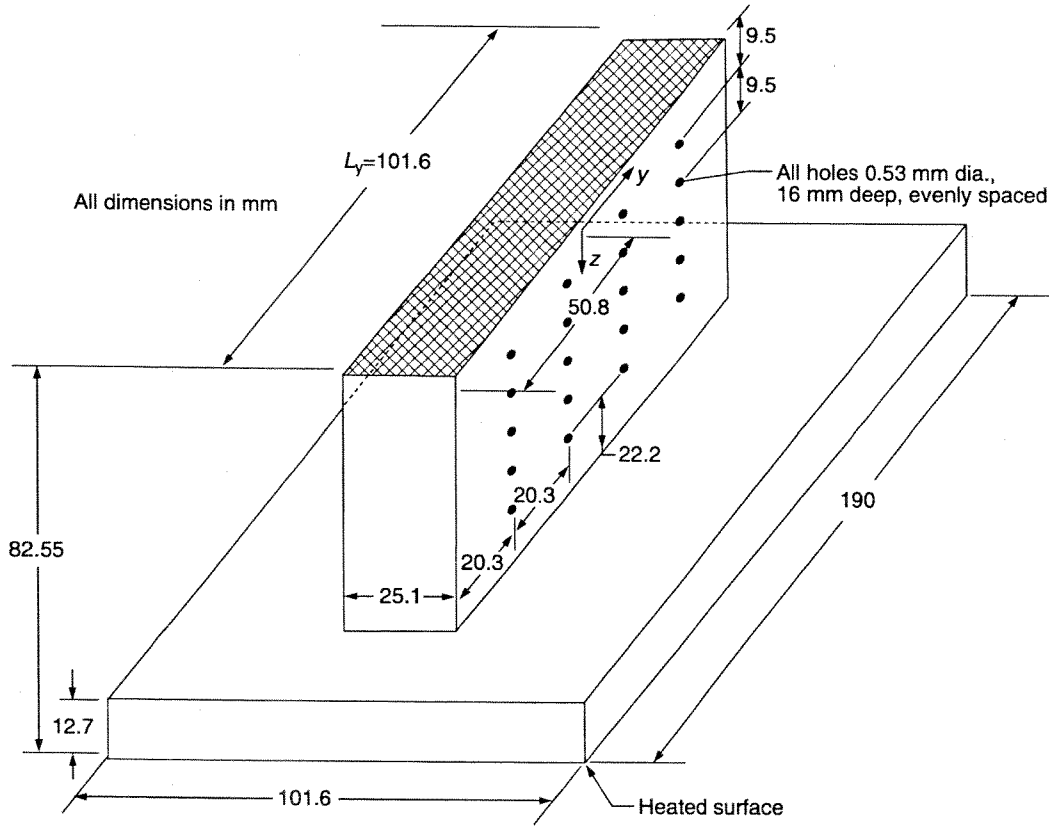


Fig. 2. OFHC copper flat test plate with cross-hatched surface and thermocouple coordinate system.

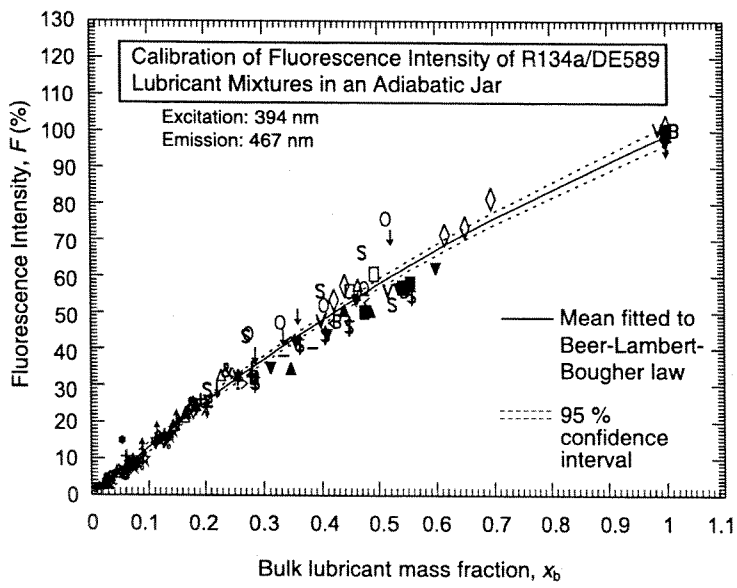


Fig. 3. Fluorescence calibration with $F=100$ for 100% DE589 jar.

fluorescence measurement method of the previous study. Because the fluorescence intensity of the present POE was significantly less than that of the previous study with mineral oil, signal noise from stray wavelengths was of the order of the POE emission. To remedy this, the spectrofluorometer was modified such that both the excitation and the emission were limited to a narrow wavelength band with interference filters as detailed in Ref. [5].

Fig. 3 shows 14 different calibration runs for the measured intensity of the fluorescence emission (F) versus the bulk lubricant mass fraction (x_b). Each calibration run, of decreasing F and x_b , is represented by a different symbol. The measurements were repeated from run to run. The solid line depicts the regression of the measured F to the Beer–Lambert–Bougher law [1] as a function of the measured x_b and the bulk liquid mixture density (ρ_b):

$$F_c = 518[1 - 10^{-9.43 \times 10^{-5} x_b \rho_b}] \quad (1)$$

The average 95% confidence interval for the lubricant mass fraction is approximately ± 0.01 (mass fraction). The width of the confidence interval is a function of the lubricant fluorescence. A greater absolute fluorescence intensity would reduce the scatter in the data. The fluorescence calibration measurements that were used to generate Eq. (1) and the pure lubricant liquid density that was measured in a pycnometer are given in Ref. [5]. The mixture densities were calculated on a linear mass weighted basis.

Because the molar mass of the lubricant is unknown, the surface excess density (Γ) is defined in this work on a mass basis as:

$$\Gamma = \rho_e x_e l_e - \rho_b x_b l_e \quad (2)$$

where the l_e is the thickness of the lubricant excess layer. Precedence for reporting the surface excess density in mass units is given by citing the work of McBain and Humphreys [14] in which they experimentally verified the Gibbs adsorption equation. A non-zero value of Γ implies that an excess layer exists on the surface.

The equation for calculating the surface excess density from the measured fluorescence emission intensity (F_m) [7] for the DE589 lubricant was slightly modified [5] to account for the temperature difference between the excess layer and the bulk fluid:

$$\begin{aligned} \Gamma &= \rho_e x_e l_e - \rho_b x_b l_e \\ &= \frac{\rho_b x_b \left(\frac{\rho_b T_c}{\rho_b T_b} - \frac{\rho_b x_b}{\rho_b T_b} \right) \left(\frac{F_m}{F_c} - 1 \right)}{\frac{l_{ob}}{l_e} \left(1 + 1.165 \frac{\epsilon}{M_L} x_b \rho_b l_b \right) \frac{\rho^{\beta(T_c - T_b)}}{l_b} - 1.165 \frac{\epsilon}{M_L} x_b \rho_b \left(\frac{F_m}{F_c} - 1 \right)} \end{aligned} \quad (3)$$

where the value of ϵ/M_L was obtained from the fluorescence calibration as $0.0646 \text{ m}^2/\text{kg}$, and the fluorescence temperature dependence coefficient (β) was experimentally determined to be 0.01 K^{-1} [5]. All of the fluid properties are evaluated at the bulk fluid temperature (T_b) with the

exception of the ρ_L, T_c , which is the pure lubricant density evaluated at the average temperature of the excess layer (T_c). If T_c and T_b are equal, Eq. (3) reduces to the original form that was given in Ref. [7]. For the measurements taken for this study, the correction to account for the temperature dependence of the fluorescence in the excess layer effected Γ by as much as 2%.

Input for Eq. (3) is as follows. The fluorescent intensity from the calibration (F_c) is obtained from Eq. (1) evaluated at the charged bulk lubricant concentration of test fluid in the boiling apparatus. The l_b is the distance between the probe and the heat transfer surface and $l_b \gg l_e$. The density of the pure lubricant is ρ_L . The ratio of the absorption of the incident excitation in the bulk to that in the excess layer (I_{ob}/I_{ob}) was obtained from the measured absorption spectrum of a 92.9/7.1 mass fraction mixture of R134a and DE589 shown in Fig. 1 of Ref. [5]. Absorption ratios for the 99.5/0.5, the 99/1.0, and the 98/2.0 mixtures were 0.950, 0.993, 0.986, respectively.

Eq. (3) was derived while assuming that the excess layer exists at a minimum thickness, i.e. the excess layer is entirely lubricant. Small excess layer mass fractions give excess layers that are unrealistically too thick. For example, the excess layer thickness ranges from 0.7 to 1.3 mm for an assumed excess layer mass fraction of 0.03. Two physical mechanisms support a thin, pure lubricant layer: (1) the preferential evaporation of the refrigerant tends to enrich the excess layer in the lubricant phase; while (2) the removal of lubricant from the surface as lubricant ‘caps’ on bubbles tends to minimize the thickness of the lubricant excess layer.

5. Experimental results

5.1. Heat transfer

The heat flux was varied between the range of 130 and 5 kW/m^2 to simulate most possible operating conditions for R134a chillers. All pool-boiling tests were taken at 277.6 K saturated conditions. The data were recorded consecutively starting at the largest heat flux and descending in intervals of approximately 4 kW/m^2 . The descending heat flux procedure minimized the possibility of any hysteresis effects on the data, which would have made the data sensitive to the initial operating conditions. Ref. [5] provides tables for the measured heat flux and wall superheat for all the data of this study.

The R134a/mixture was prepared by charging the test chamber (Fig. 1) with pure R134a to a known mass. Next, a measured mass of DE589 was injected with a syringe through a port in the test chamber. The lubricant was mixed with R134a by flushing pure R134a through the same port where the lubricant was injected. All compositions were determined from the masses of the charged components and are given on a mass percent basis. The maximum uncertainty of the composition measurement is

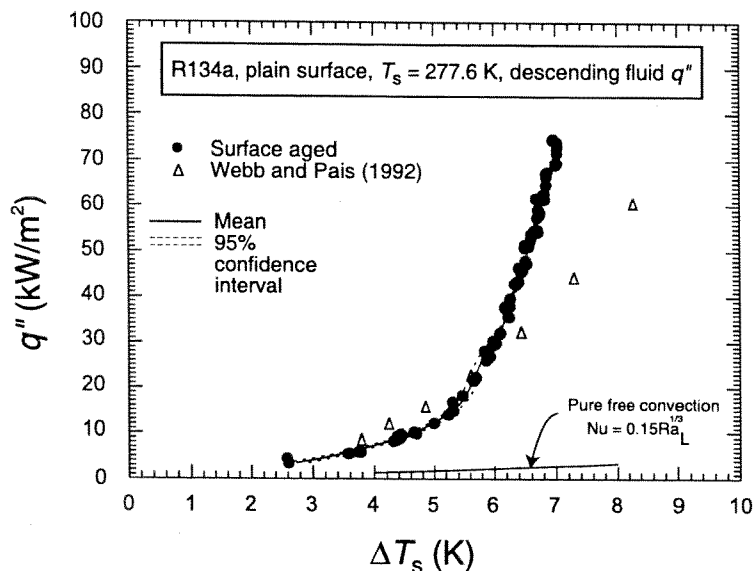


Fig. 4. Pure R134a boiling curve for plain surface.

approximately 0.02%, e.g. the range of a 2.0% composition is between 1.98 and 2.02%.

Fig. 4 is a plot of the measured heat flux (q'') versus the measured wall superheat ($T_w - T_s$) for pure R134a at a saturation temperature of 277.6 K. The closed circles represent 6 days of boiling measurements made over a period of approximately 2 weeks. 'Break-in' data taken during the first 3 days of testing, before the surface had fully 'aged,' are not shown on the figure, but are given in Ref. [5]. The aging effect has previously been observed for this surface for the tests immediately following cleaning and installation [9]. The present surface was cleaned prior to installation in the test apparatus sequentially with acetone, Tarnex, hot tap water, and acetone. Marto and Lepere [13] have also observed a surface aging effect on pool boiling data that was sensitive to initial surface conditioning and fluid properties.

The solid lines shown in Fig. 4 are cubic best-fit regressions or estimated means of the data. Nine of the 144 measurements were removed before fitting because they were identified as 'outliers' based on having both high influence and high leverage [2]. Table 1 gives the constants for the cubic regression of the superheat versus the heat flux for all of the fluids tested here. The residual standard deviation of the regressions—representing the proximity of the data to the mean—are between 0.04 and 0.4 K. The dashed lines to either side of the mean represent the lower and upper 95% simultaneous (multiple-use) confidence intervals for the mean. From the confidence intervals, the expanded uncertainty of the estimated mean wall superheat was 0.1 and 0.04 K for superheats less than and greater than 6 K, respectively.

Fig. 4 also provides the smooth tube boiling data of Ref. [17] at the same saturation temperature as the present tests.

The largest differences between the smooth tube and the data of [17] and the present flat plate measurements are found at the extremes of the data set. For the same superheat [17], the smooth tube heat flux is 60% greater than and 40% less than the measured heat flux for the flat plate at 10 and 70 kW/m², respectively. Averaged over the entire heat flux range of the data the [17] heat flux is 18% less than the present flat plate heat flux for the same superheat. For further reference, Fig. 4 shows the predictions from a free convection correlation for a horizontal plate with the heated surface facing upward, which was recommended by Ref. [3]. The natural convection heat flux predictions range from 10 to 4% of the boiling heat fluxes for the same wall superheat.

Fig. 5 plots the measured heat flux (q'') versus the measured wall superheat ($T_w - T_s$) at a saturation temperature of 277.6 K for the (99.5/0.5), (99/1), and the (98/2) R134a/DE589 mixtures. The mean of the pure R134a 'aged data' is plotted as a dashed line. Comparison of the 99.5/0.5 mixture boiling curve to the mean R134a boiling curve shows that they intersect at a superheat of approximately 5.8 K. For mean superheats between 4 and 5.8 K, the 99.5/0.5 mixture exhibits an enhancement in the heat flux as compared to the pure refrigerant. In contrast, the pure R134a heat flux is greater than that of the 99.5/0.5 mixture for superheats greater than 5.8 K. Apparently, the lubricant enhances the site density and, in turn, the heat transfer for superheats between 4 and 5.8 K. This enhancement mechanism is ineffective at superheats greater than 5.8 K because nearly all of the available sites have been activated leaving no opportunity for improvement. For superheats greater than 5.8 K, the degradation exhibited by the 99.5/0.5 mixture results from the decrease in bubble size associated with the lubricant.

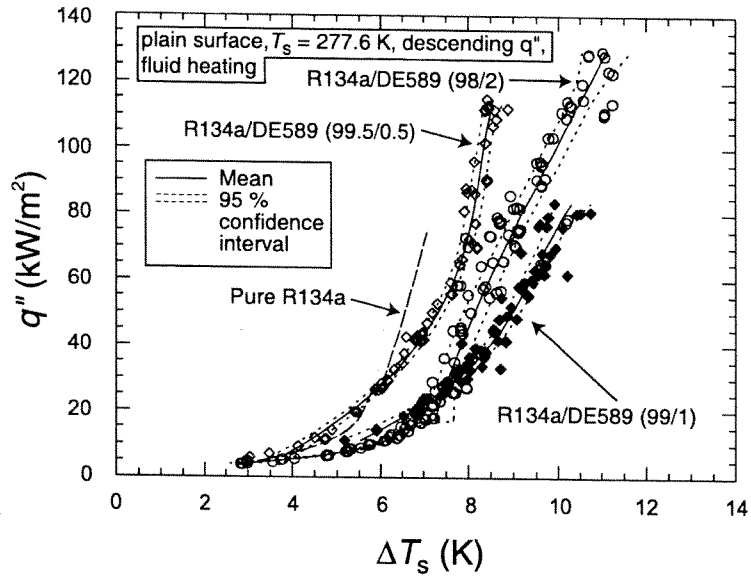


Fig. 5. Three R134a/DE589 mixture boiling curves for plain surface.

Fig. 5 shows that the boiling performance of the 99/1 mixture for all superheats is less than that of both the pure R134a and the 99.5/0.5 mixture. In addition, the scatter in the 99/1 mixture data is marginally larger than that for the 99.5/0.5 mixture given that the residual standard deviation is 0.19 and 0.26 K, respectively. The scatter of the 98/2 mixture is the largest of the fluids tested being 0.39 K. The general trend of increasing measurement variability with increasing lubricant concentration is consistent with that observed by Refs. [7,9]. The boiling performance of the 98/2 mixture does not follow the trend of decreasing performance

with increasing lubricant mass fraction for heat fluxes greater than approximately 30 kW/m². For a given superheat for heat fluxes greater than 30 kW/m², the heat flux of the 98/2 mixture is between that of the 99.5/0.5 and the 99/1 mixtures. This characteristic is not likely due to the larger heat flux range of the 98/2 measurements because some of the data with the most favorable performance was taken at a starting heat flux of 80 kW/m², which coincides with the starting heat flux of much of the 99/1 mixture data. The observed enhancement associated with the increase in lubricant mass fraction to 2% may likely have been induced

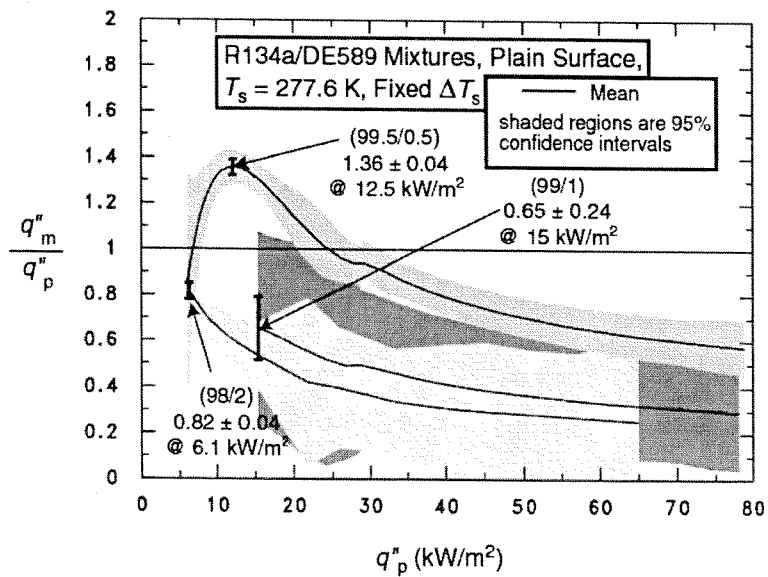


Fig. 6. Three R134a/DE589 mixture heat fluxes relative to pure R134a for a plain surface.

by a significant increase in site density without a significant loss in bubble size as compared to the 1% lubricant concentration.

A more detailed comparison of the mixture and the pure fluid heat transfer performance is given in Fig. 6. Fig. 6 plots the ratio of the mixture to the pure R134a heat flux (q''_m/q''_p) versus the pure R134a heat flux (q''_p) at the same wall superheat. A heat transfer enhancement exists where the heat flux ratio is greater than one and the 95% simultaneous confidence intervals (depicted by the shaded regions) do not include the value one. Fig. 6 shows that the R134a/DE589 (99.5/0.5) mixture exhibits an enhancement over pure R134a for heat fluxes between approximately 7 and 22 kW/m². The maximum heat flux ratio for the 99.5/0.5 mixture was 1.36 ± 0.04 at 12.5 kW/m². The average heat flux ratio for the R134a/DE589 (99.5/0.5) mixture from approximately 6 to 21 kW/m² was 1.24. The average heat flux ratio from approximately 6 to 81 kW/m² was 0.84.

Fig. 6 shows that the R134a/DE589 (99/1) mixture exhibits a heat transfer degradation for all heat fluxes shown. The maximum heat flux ratio for the 99/1 mixture was 0.65 ± 0.24 at a pure R134a heat flux of 15 kW/m². The average heat flux ratio for the R134a/DE589 (99/1) mixture from approximately 15 to 82 kW/m² was 0.4.

Fig. 6 shows that the R134a/DE589 (98/2) mixture exhibits a degradation for all the heat fluxes that were tested. The maximum heat flux ratio of 0.82 ± 0.04 was observed at pure R134a heat flux of 6.1 kW/m². The average heat flux ratio for the R134a/DE589 (98/2) mixture from approximately 6 to 88 kW/m² was 0.34.

For the comparisons made in Fig. 6, the available range of pure R134a heat fluxes corresponds to heat fluxes less than 50 kW/m² for the 99.5/0.5 mixture and to heat fluxes less than 25 kW/m² for the 99/1 and the 98/2 mixtures. In order to

examine the relative magnitudes of the mixture heat fluxes greater than 50 kW/m², Fig. 7 normalizes the mixture heat flux relative to that of the 98/2 mixture ($q''_{2\%}$) rather than pure R134a heat flux (at the same wall superheat). Fig. 7 illustrates that the boiling performance of the 99.5/0.5 mixture averaged between 5 and 60 kW/m² is approximately 94% greater than that of the 98/2 mixture. The maximum heat flux ratio for the 99.5/0.5 mixture relative to the 98/2 mixture is 2.6 ± 0.01 at 10 kW/m². The heat flux ratio of the 99/1 mixture has a maximum of 1.35 ± 0.09 at 11 kW/m² and an average of approximately 0.91 between 8 and 65 kW/m².

5.2. Fluorescence

Although the heat flux was varied between the range of 130 and 5 kW/m², fluorescence measurements were limited between 50 and 15 kW/m² to limit the time required to quench the boiling below the fluorescence probe. Bubbles under the probe would have misdirected the incident excitation and the fluorescent emission resulting in a significantly reduced and erroneous emission signal. Consequently, the boiling was quenched prior to making fluorescent emission measurements. Fluorescence intensity measurements were made with respect to time while no bubbles were visible below the probe. These measurements were extrapolated to a time just before quenching to obtain the fluorescence of the surface during boiling just prior to quenching giving the intensity during boiling. Errors associated with the extrapolation procedure depend largely on the slope of the fluorescent signal with respect to time. In general, the slope of the fluorescent signal with respect to time was relatively small indicating that the diffusion of the lubricant from the surface into the bulk at the time of measurement had not occurred to a great extent. In addition,

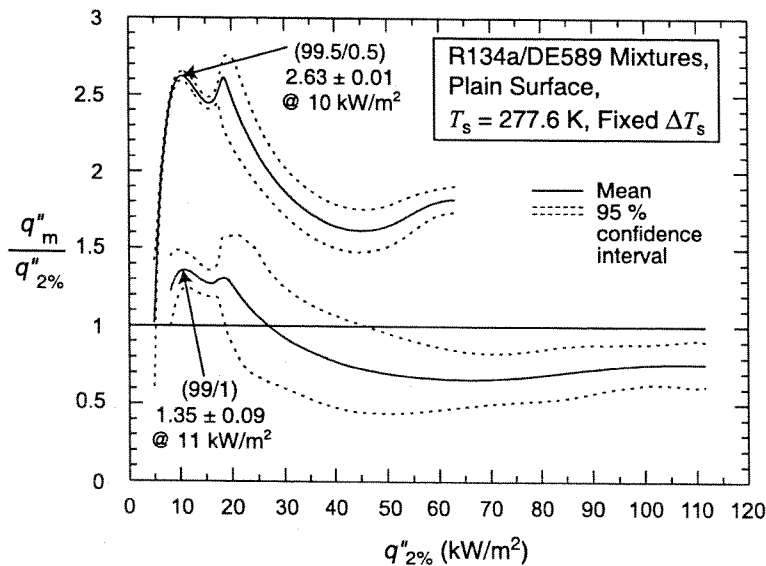


Fig. 7. Two R134a/DE589 mixture heat fluxes relative to R134a/DE589 (98/2) for a plain surface.

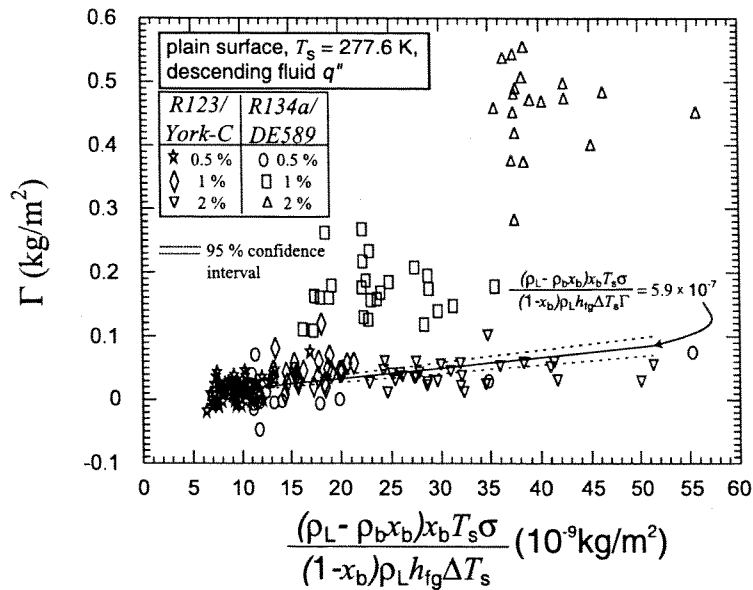


Fig. 8. Lubricant excess surface density for six refrigerant/lubricant mixtures as a function of non-dimensional excess surface density as defined in Ref. [4].

the variation of the fluorescence over the period of measure was generally considerably smaller than the scatter of between-run extrapolated measurements. As a result, the errors introduced by the extrapolating procedure were considered negligible.

Fig. 8 shows the lubricant excess surface density measurements for the three R134a/DE589 mixtures as calculated with Eq. (3)² versus the excess property group developed in Ref. [4] from R123/York-C Γ measurements taken in Ref. [7]. Ref. [5] provides the raw extrapolated fluorescence intensity measurements that were used in Eq. (3). The excess property group was used to derive the following constant for the inverse of the dimensionless pool boiling refrigerant/lubricant excess surface density ($\hat{\Gamma}$):

$$(\hat{\Gamma})^{-1} = \frac{(\rho_L - \rho_b x_b) x_b T_s \sigma}{(1 - x_b) \rho_L h_{fg} \Delta T_s \Gamma} = 5.9 \times 10^{-7} \quad (4)$$

Eq. (4) was a key component of the refrigerant/lubricant pool boiling heat transfer model present in Ref. [4] and essentially represents the slope of the R123/York-C data in Fig. 8. Although, Eq. (4) agrees well with the R123/York-C measurements, it fails to predict the Γ measurements for the R134a/DE589 (99/1) and (98/2) mixtures. A probable reason for this is that larger reduced pressure as compared to R123, and thus, smaller diameter bubbles associated with R134a cannot remove the lubricant from the wall as well as the larger R123 bubbles. The consequence of the reduced effectiveness of lubricant removal is that the R134a Γ is

larger than what would be expected for R123 with all other conditions given in Eq. (4) being fixed. Consequently, it is likely that Eq. (4) should include a reduced pressure term to account for the reduced lubricant removal effectiveness at larger reduced pressure.

In light of this, two modifications were made to the $\hat{\Gamma}$ given in Eq. (4) so that both R123 and R134a Γ measurements could be predicted with a single relationship. First a reduced pressure ($P_r = P/P_c$) term similar to that given by Refs. [15,12] was included to capture the effects of pressure on boiling. The second modification was to allow the thickness of the lubricant on the bubble to vary with bulk lubricant mass fraction. Because the $\hat{\Gamma}$ was developed from a physical model based on a lubricant mass balance on the bubble, the thickness of the lubricant on the bubble is of primary importance. In the original model, the thickness was assumed to be constant. The present modification allows for a small variation of the lubricant thickness on the bubble with respect to mass fraction. The complete derivation including the present modifications to $\hat{\Gamma}$ is given in Ref. [5]. The inverse of the modified $\hat{\Gamma}$ which accounts for the effects of reduced pressure and variable lubricant thickness on the bubble is:

$$\begin{aligned} (\hat{\Gamma})^{-1} &= \frac{(\rho_L - \rho_b x_b) x_b^{1.8} T_s \sigma P_r}{(1 - x_b) \rho_L h_{fg} \Delta T_s \Gamma} \\ &= 2.8 \times 10^{-10} \pm 0.2 \times 10^{-10} \quad (5) \end{aligned}$$

Eq. (5) was obtained from a single regression of the present R134a/DE589 and the R123/York-C measurements from Ref. [7]. Fig. 9 shows that Eq. (5) represents the measured Γ for both the R134a/DE589 and the R123/York-C

² Using extrapolated fluorescence intensity measurements as described above.

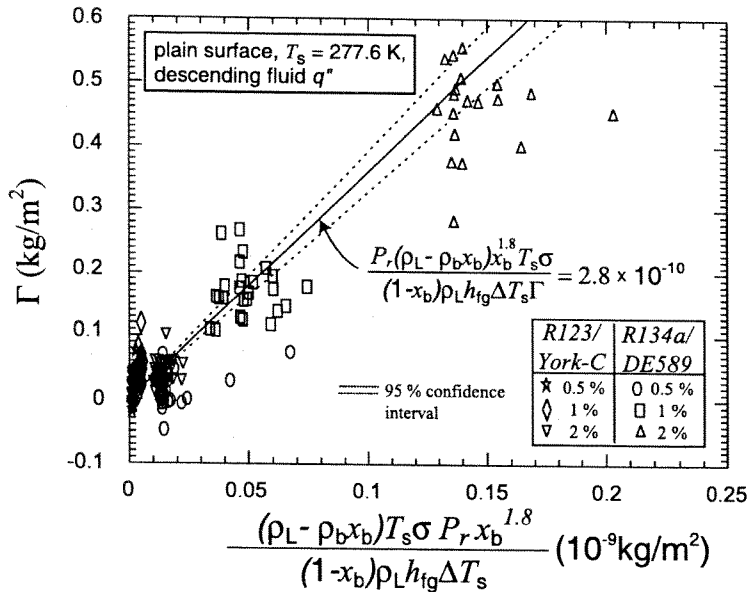


Fig. 9. Lubricant excess surface density for six refrigerant/lubricant mixtures as a function of pressure-corrected non-dimensional excess surface density.

mixtures to an average residual standard deviation of 0.1 kg/m². Consequently, the modified \hat{T} can be used to broaden the applicability of the pool boiling model to refrigerants and lubricants other than R123 and York-C.

6. Conclusions

A newly developed fluorescent measurement technique was used to investigate the effect of bulk lubricant concentration on the lubricant excess layer during boiling of R134a and a polyolester lubricant (DE589). A spectrofluorometer was specially adapted for use with a bifurcated optical bundle so that fluorescence measurements could be made perpendicular to the heat transfer surface. The heat transfer surface was a horizontal, roughened, copper flat plate. The lubricant excess surface density was shown to increase with respect to a modified dimensionless lubricant excess surface density parameter.

The boiling heat transfer measurements were simultaneously taken with the fluorescence measurements. The heat transfer data shows that the lubricant excess layer causes an average enhancement of the heat flux of approximately 24% for the 0.5% lubricant mass fraction mixture relative to pure R134a heat fluxes between 5 and 20 kW/m². Conversely, both the 1 and 2% lubricant mass fraction mixtures experienced an average degradation of approximately 60% in the heat flux relative to pure R134a heat fluxes between approximately 4 and 20 kW/m².

The lubricant excess surface density measurements were used to modify an existing dimensionless excess surface

density parameter so that it is valid for different reduced pressures. The dimensionless parameter is a key component for a refrigerant/lubricant pool-boiling model given in the literature by the author. In support of improving the boiling model, both the excess measurements and heat transfer data are provided for pure R134a and three R134a/lubricant mixtures at 277.6 K. This study is an effort toward generating data that can be used to support a boiling model that can be used to predict whether lubricants degrade or improve boiling performance.

Acknowledgements

This work was jointly funded by NIST and the U.S. Department of Energy (project no. DE-01-95CE23808.000 modification #A004) under Project Manager Arun Vohra. Thanks go to the following people for their constructive criticism of the first draft of the manuscript: Mr J. Bogart, Dr W. Payne, and Dr P. Domanski. The author would also like to express appreciation to Mr J. Fry, and Mr G. Glaeser of the NIST Building Environment Division for data collection. Furthermore, the author extends appreciation to Dr W. Guthrie and Mr A. Heckert of the NIST Statistical Engineering Division for their consultations on the uncertainty analysis. Special thanks goes to Dr T. Vorburger of the NIST Precision Engineering Division for making the roughness measurements of the crosshatch surface. The DE589 lubricant that was donated by Dr S. Randles and Dr T. Dekleva of ICI is much appreciated.

References

- [1] J.P. Amadeo, C. Rosén, T.L. Pasby, *Fluorescence spectroscopy an introduction for biology and medicine*, Marcel Dekker, New York, 1971. p. 153.
- [2] D.A. Belsley, E. Kuh, R.E. Welsch, *Regression diagnostics: identifying influential data and sources of collinearity*, Wiley, New York, 1980.
- [3] F.P. Incropera, D.P. DeWitt, *Fundamentals of heat and mass transfer*, 2nd ed, Wiley, New York, 1985.
- [4] M.A. Kedzierski, A semi-theoretical model for predicting R123/lubricant mixture pool boiling heat transfer, *Int J Refrig* 26 (2003) 337–348.
- [5] M.A. Kedzierski, Effect of bulk lubricant concentration on the excess surface density during R134a pool boiling with extensive measurement and analysis details, US Department of Commerce, Washington, DC, 2003. [NISTIR 7051].
- [6] M.A. Kedzierski, Use of fluorescence to measure the lubricant excess surface density during pool boiling, *Int J Refrig* 25 (2002) 1110–1122.
- [7] M.A. Kedzierski, Effect of bulk lubricant concentration on the excess surface density during R123 pool boiling, *Int J Refrig* 25 (2002) 1062–1071.
- [8] M.A. Kedzierski, Use of fluorescence to measure the lubricant excess surface density during pool boiling, US Department of Commerce, Washington, DC, 2001. [NISTIR 6727].
- [9] M.A. Kedzierski, Effect of bulk lubricant concentration on the excess surface density during R123 pool boiling, US Department of Commerce, Washington, DC, 2001. [NISTIR 6754].
- [10] M.A. Kedzierski, Enhancement of R123 pool boiling by the addition of hydrocarbons, *Int J Refrig* 23 (2000) 89–100.
- [11] M.A. Kedzierski, Calorimetric and visual measurements of R123 pool boiling on four enhanced surfaces, US Department of Commerce, Washington, DC, 1995. [NISTIR 5732].
- [12] K. Nishikawa, K. Urakawa, An experiment of nucleate boiling under reduced pressure, *Memoirs Faculty Eng, Kyushu Univ* 19 (3) (1960) 63–71.
- [13] P.J. Marto, V.J. Lepere, Pool boiling heat transfer from enhanced surfaces to dielectric fluids, *ASME J Heat Transfer* 104 (1982) 292–299.
- [14] J.W. McBain, C.W. Humphreys, The microtome method of the determination of the absolute amount of adsorption, *J Chem Phys* 36 (1932) 300–311.
- [15] R. Semeria, Quelques Resultats sur le Mecanisme de l'Ebullition, *J de l'Hydraulique de la Soc Hydrotechnique de France* 7 (1962).
- [16] K. Stephan, Influence of oil on heat transfer of boiling refrigerant 12 and refrigerant 22, *XI Int Congr Refrig* 1 (1963) 369–380.
- [17] R.L. Webb, C. Pais, Nucleate pool boiling data for five refrigerants on plain, integral-fin and enhanced tube geometries, *Int J Heat Mass Transfer* 35 (8) (1992) 1893–1904.